ACS chemical biology

Articles

pubs.acs.org/acschemicalbiology

Androgen Receptor Antagonism by Divalent Ethisterone Conjugates in Castrate-Resistant Prostate Cancer Cells

Paul M. Levine,[†] Eugine Lee,[‡] Alex Greenfield,[§] Richard Bonneau,[§] Susan K. Logan,[‡,⊥] Michael J. Garabedian,[⊥,∥] and Kent Kirshenbaum*[,†]

[†]Department of Chemistry and [§]Center for Genomics and Systems Biology, New York University, New York, New York 10003, United States

[‡]Department of Biochemistry and Molecular Pharmacology, [⊥]Department of Urology, and [∥]Department of Microbiology, NYU Langone School of Medicine, New York, New York 10016, United States

Supporting Information

ABSTRACT: Sustained treatment of prostate cancer with androgen receptor (AR) antagonists can evoke drug resistance, leading to castrate-resistant disease. Elevated activity of the AR is often associated with this highly aggressive disease state. Therefore, new therapeutic regimens that target and modulate AR activity could prove beneficial. We previously introduced a versatile chemical platform to generate competitive and non-competitive multivalent peptoid oligomer conjugates that modulate AR activity. In particular, we identified a linear and a cyclic divalent ethisterone conjugate that exhibit potent anti-proliferative properties in LNCaP-abl cells, a model of castrate-resistant prostate cancer. Here, we characterize the mechanism of action of these compounds utilizing confocal microscopy, time-resolved fluorescence resonance energy transfer, chromatin immunoprecipitation, flow cytometry, and microarray analysis. The linear conjugate competitively blocks AR action by inhibiting DNA binding. In addition, the linear conjugate does not promote AR nuclear localization or co-activator binding. In contrast, the cyclic conjugate promotes AR nuclear localization and induces cell-cycle arrest, despite its inability to compete against endogenous ligand for binding to AR *in vitro*. Genome-wide expression analysis reveals that gene transcripts are differentially affected by treatment with the linear or cyclic conjugate. Although the divalent ethisterone conjugates share extensive chemical similarities, we illustrate that they can antagonize the AR *via* distinct mechanisms of action, establishing new therapeutic strategies for potential applications in AR pharmacology.

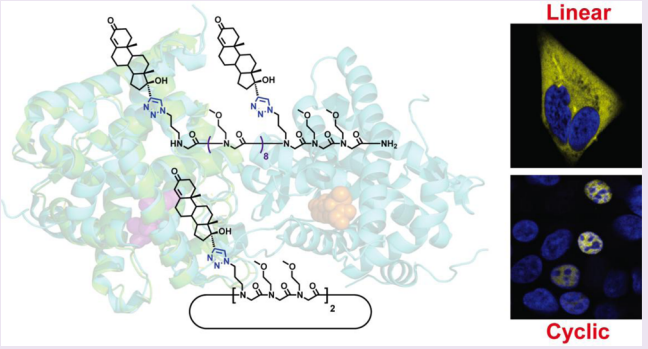

The tendency of prostate cancer tumors to develop drug resistance presents a critical challenge in androgen receptor (AR) pharmacology. Patients diagnosed with localized or metastatic prostate cancer usually undergo androgen deprivation therapy in conjunction with AR antagonists, such as bicalutamide, to block receptor signaling.[1,2] Drug resistance can therefore manifest in patients following long-term treatment, resulting in the development of castrate-resistant prostate cancer.[3] While the molecular mechanisms responsible for progression to this currently incurable disease state are not fully understood, evidence suggests that elevated AR activity plays a central role in stimulating tumor growth.[4,5] Thus, there is increasing interest in identifying new therapies that specifically target and modulate AR activity.

Androgens are steroid hormones that mediate their effects primarily through the AR to play a fundamental role in a wide range of physiological processes, including prostate growth and differentiation.[6−8] The AR is a ligand-dependent transcription factor that is stabilized in the cytoplasm by chaperone proteins.[9] Displacement of the chaperones by the native androgen dihydrotestosterone (DHT) activates the AR and induces a conformational change that brings the N- and C-termini into close proximity.[10,11] Following activation, the AR undergoes dimerization, phosphorylation, and translocation into the nucleus where it can bind to palindromic 5′-TGTTCT-3′ consensus sequences (androgen response elements).[12,13] Subsequently, RNA polymerase II and necessary cofactors, including LxxLL or FxxLF motif-containing proteins, are recruited to regulate gene expression.[14]

Androgens that function through the AR can also promote prostate cancer growth and development.[15] Competitive antagonism of the AR has been the major focus of AR-based drug discovery. Typically, chemical screening identifies small molecules that competitively target the ligand binding domain (LBD) and disrupt AR activity by inhibiting co-activator recruitment, DNA binding, or nuclear localization.[16] While effective at temporarily regressing tumor burden, sustained treatment can result in drug resistance that arises through a

Received: May 21, 2012
Accepted: July 25, 2012
Published: August 7, 2012

variety of mechanisms, including gain of function mutations, production of shortened AR transcripts, new fusion gene products, and cross-talk with other signaling pathways, leading to castrate-resistant prostate cancer.[17,18] Unfortunately, current therapeutic options for castrate-resistant prostate cancer only demonstrate modest survival benefits and most patients succumb to their disease within a few months.[19]

In order to circumvent drug resistance, new therapeutic agents for prostate cancer should ideally possess mechanisms of action that are distinct from those of current approaches. Recent evidence suggests that allosteric regulation of AR activity through non-competitive mechanisms may be an effective strategy for independent or synergistic treatment of castrate-resistant prostate cancer.[20,21] We have introduced a versatile oligomer platform that allows rational design of multivalent conjugates to specifically target and modulate AR activity through competitive or non-competitive mechanisms.[22] The use of multivalency in chemical biology has emerged as a powerful tool to enhance binding affinity and specificity for corresponding biomolecular targets.[23−26] Multivalent displays are capable of modulating multimeric protein receptors through multisite binding contacts, which can be otherwise difficult to achieve by small molecules.[27,28] In addition, utilizing modular oligomer frameworks to display ligands in a multivalent fashion can enable control over important physicochemical features of the products, including solubility and cellular uptake.[29−31]

N-Substituted glycine oligomers, or "peptoids", have recently been explored as multivalent platforms for the design of constructs capable of modulating the activity of different biomacromolecules.[31−33] Peptoids are composed of tertiary amide linkages, offering favorable pharmacological characteristics relative to peptides, including proteolytic stability and enhanced cellular permeability (Figure 1).[34,35] The ability to incorporate extensive chemical diversity into the peptoid side chains permits design strategies that allow for a wide range of functions, such as enantioselective catalysis, molecular recognition, antimicrobial activity, intracellular delivery, and antitumor activity *in vivo*.[36−42] Solid-phase synthesis of sequence-specific peptoid oligomers provides access to monodisperse products, a distinct advantage over other multivalent display platforms (*e.g.*, random copolymers or dendrimers).[43,44] In addition, the conformation of oligomeric scaffolds can be constrained to enhance ligand−receptor binding interactions.[27,45]

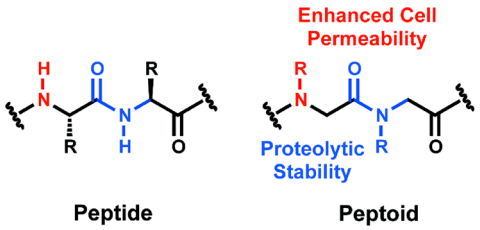

Figure 1. Comparison of peptide and peptoid structures. Peptoids feature tertiary amide linkages, engendering proteolytic stability and enhanced cell permeability.

We have previously described the synthesis of a linear and a cyclic peptoid oligomer incorporating azido-alkyl functionalized side chains at defined positions in the oligomer sequence.[22,46,47] Following oligomerization (and cyclization as required), Cu-catalyzed azide−alkyne [3 + 2] cycloaddition (CuAAC) reactions were employed to conjugate bioactive ethisterone ligands along the oligomer backbone, generating either a linear divalent dodecamer peptoid conjugate (**1**) or a cyclic divalent hexamer peptoid conjugate (**2**) (Figure 2 and Supplementary Figure 1).[48] In an effort to enhance overall water solubility, all other intervening positions in the peptoid sequence included the hydrophilic submomomer *N*-(methoxyethyl)glycine. It is important to note that we have evaluated cell permeability of similar oligomer steroid-conjugates (*i.e.*, estradiol conjugates, instead of ethisterone conjugates). A linear version of the divalent hexamer conjugate as well as an analogous divalent dodecamer were shown to be cell-permeable.[31] On the basis of previous studies, the expectation is that cyclic oligomers would typically exhibit enhanced cell permeability and therefore that both linear and cyclic steroid conjugates would permit efficient cell uptake.[49,50]

Initial screening of conjugates **1** and **2** revealed that they modulate AR activity through competitive and non-competitive mechanisms, respectively. Additionally, conjugates **1** and **2** displayed anti-proliferative activity in LNCaP-abl cells, a cell culture model of castrate-resistant prostate cancer that proliferates in low hormone conditions.[22,51] The conjugates exhibited potent anti-proliferative effects at a concentration of 1 μM. Importantly, cytotoxicity was not observed in non-AR expressing human embryonic kidney (HEK293) cells or AR-deficient prostate cancer (PC3) cells, suggesting conjugates **1** and **2** selectively target the AR in LNCaP-abl cells. These results highlighted the potential biomedical significance of multivalent peptoid conjugates for castrate-resistant prostate cancer. Here, we investigate the biological mechanism of action

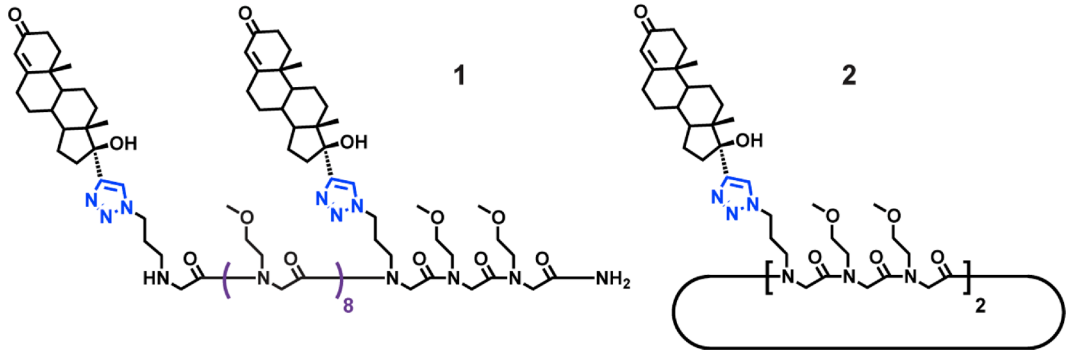

Figure 2. Chemical structures of linear divalent ethisterone-peptoid conjugate **1** and cyclic divalent ethisterone-peptoid conjugate **2**. Conjugate **1** competes with DHT for binding to the Androgen Receptor (AR), whereas conjugate **2** does not.[22]

through which conjugates **1** and **2** exhibit their potent antiproliferative effects in this aggressive disease state.

RESULTS AND DISCUSSION

Effect on AR Protein Expression and Cellular Localization. We first evaluated if conjugate **1** or **2** can induce AR degradation within the cell, as previous studies of AR antagonists have reported the induction of receptor degradation *in vivo*.[52] Cellular extracts of LNCaP-abl cells treated with either conjugate **1** or **2** were prepared and immunoblotted for AR (Figure 3A). Conjugates **1** and **2** exhibited no significant effect on AR protein levels, relative to control treatments. Thus, conjugates **1** and **2** do not induce AR degradation.

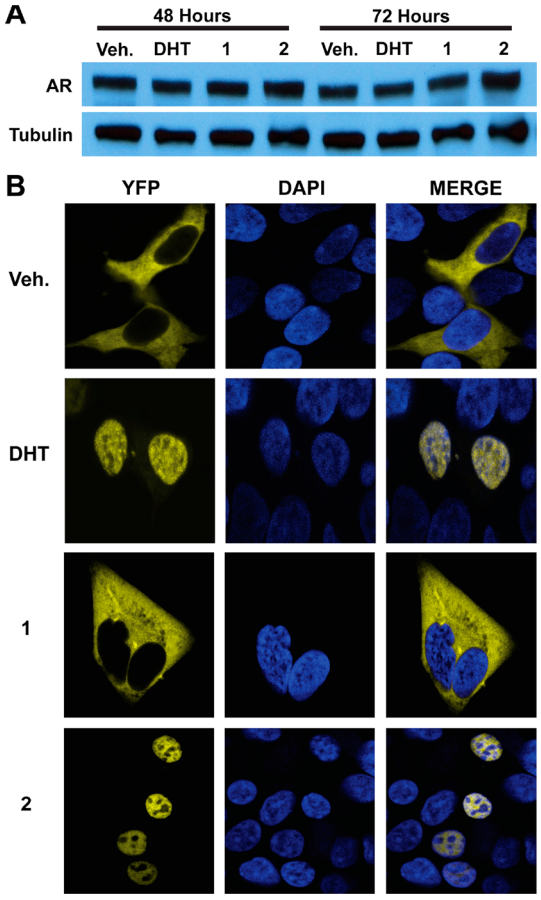

Figure 3. Conjugates **1** and **2** differentially effect AR cellular localization. (A) Peptoid conjugates do not induce AR degradation. AR protein expression in treated LNCaP-abl cells with tubulin as a loading control (Veh., EtOH-treated cells; DHT, 10 nM; conjugate **1** or **2**, 1 μM). Treatment times (h) are shown above the respective lanes. (B) Cellular localization of AR in treated HEK293 cells transfected with an AR fluorescent protein hybrid (Veh., EtOH-treated cells; DHT, 1 nM; conjugate **1** or **2**, 1 μM). The yellow fluorescent protein (YFP) and 4,6-diamidino-2-phenylindole (DAPI) channels represent the localization of the AR fusion protein and the cell nuclei, respectively.

To explore the cellular localization of AR in the presence and absence of conjugates **1** or **2**, confocal microscopy was conducted utilizing an AR fluorescent protein hybrid (Figure 3B).[53] In the absence of native ligand, AR was diffusely distributed in the cytoplasm. Upon treatment with DHT, AR accumulates in the nucleus as expected. Unlike DHT, conjugate **1** does not promote AR nuclear localization. Interestingly, and in contrast to conjugate **1**, conjugate **2** evokes AR nuclear localization. This suggests conjugates **1** and **2** are eliciting distinct modes of AR antagonism.

Modulation of AR Nuclear Function. An *in vitro* time-resolved fluorescence resonance energy transfer (TR-FRET) assay was utilized to determine if conjugates **1** or **2** promote binding between AR and co-activator proteins. In this assay, the interaction between GST-tagged AR-LBD and a FxxLF co-activator peptide (VESGSSR**FMQLF**MANDLLT) is monitored in the presence of ligand by a TR-FRET signal between a terbium-labeled AR-specific anti-GST antibody and a fluorescein-labeled AR FxxLF co-activator peptide.[54] Binding of agonist to the AR-LBD induces a conformational change to helix 12 (a co-activator protein binding site), resulting in the high affinity recruitment of the FxxLF co-activator peptide. Upon excitation, energy is transferred from the terbium-labeled anti-GST antibody to the fluorescein-labeled co-activator peptide, and a TR-FRET signal is detected. In the presence of anti-androgens, helix 12 can adopt a conformation that impairs co-activator peptide binding, resulting in a decrease of the TR-FRET signal.[16] We confirmed that DHT promotes a dose-dependent interaction between AR and the FxxLF motif-containing peptide, indicative of high affinity co-activator binding (Figure 4A). As expected for an antiandrogen, the standard AR monotherapy bicalutamide partially promotes binding between AR and the co-activator peptide.[55] Conjugate **2** induced a similar dose response to bicalutamide, suggesting partial recruitment of the co-activator peptide (Figure 4A and Supplementary Figure 2). Conjugate **1** does not promote binding between AR and the fluorescein-labeled co-activator peptide.

To assess whether conjugates **1** or **2** disrupt binding between AR and DNA, chromatin immunoprecipitation (ChIP) experiments were conducted. In a positive control experiment, the synthetic competitive AR agonist R-1881 promoted AR recruitment to the prostate-specific antigen (PSA) enhancer, a well characterized androgen-regulated gene (Figure 4B).[56] Upon co-treatment with R-1881 and either conjugate **1** or **2**, the occupancy of AR to the PSA enhancer was reduced, indicating that conjugates **1** and **2** inhibit binding between AR and DNA. Conjugate **1** likely inhibits AR recruitment to the PSA enhancer because it does not promote AR nuclear localization or co-activator binding. Conjugate **1** blocked AR recruitment to the PSA enhancer at both 4 and 16 h, whereas this effect was only observed at the 16 h time point for conjugate **2**. Conjugate **2** does not compete directly with R-1881 for binding, and thus the time-course of conjugate **2** in the presence of R-1881 may be slow to elicit a biological response. This is consistent with previous studies using ChIP analysis with non-competitive antagonists.[18] As expected in control ChIP experiments, specific binding of AR in response to R-1881 is not observed upstream of the PSA enhancer, confirming the specificity of AR binding at the PSA enhancer (Supplementary Figure 3).

Cell-Cycle Distribution. We analyzed cell-cycle distribution of LNCaP-abl cells treated with either conjugate **1** or **2** utilizing fluorescence-activated cell sorting (FACS) analysis. These studies provide a quantitative assessment of normal and apoptotic nuclei along with cell distribution in the G_0/G_1, S, and G_2/M phases of the cell-cycle. Conjugate **1** showed a modest increase in the G_0/G_1 phase, relative to vehicle treatment (Figure 4C and Supplementary Figure 4). In

dx.doi.org/10.1021/cb300332w | *ACS Chem. Biol.* 2012, 7, 1693–1701

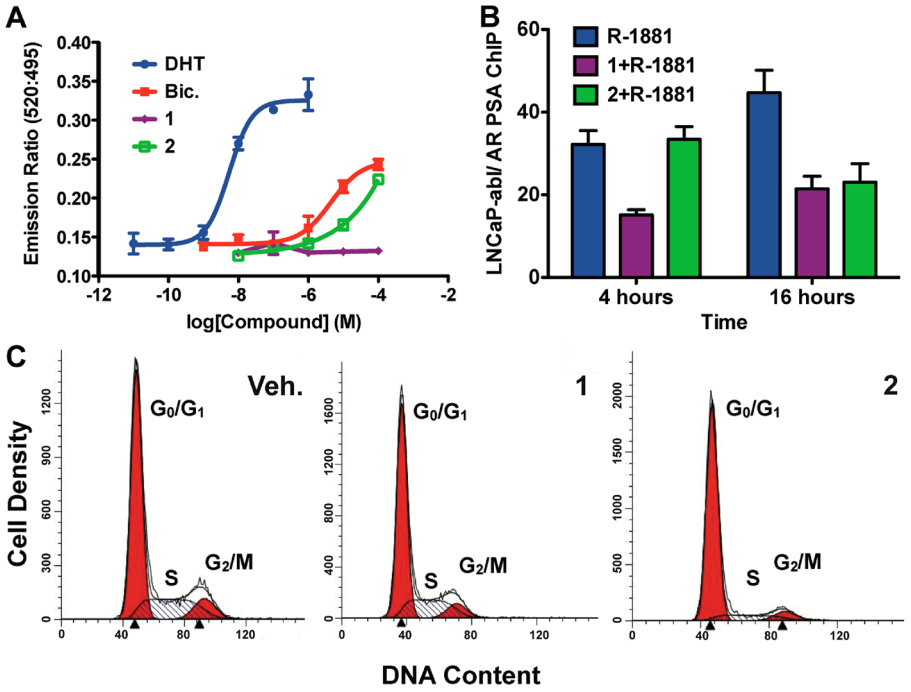

Figure 4. Conjugates **1** and **2** disrupt co-activator peptide recruitment and DNA binding. Conjugate **2** also induces cell cycle arrest. (A) *In vitro* time-resolved fluorescence resonance energy transfer (TR-FRET) analysis of the interaction between purified GST-tagged AR-LBD, terbium-labeled AR-specific anti-GST antibody, and fluorescein-labeled AR FxxLF co-activator peptide (increasing concentrations of DHT, Bicalutamide (Bic.), and Conjugate **1** or **2** were evaluated). The TR-FRET signal intensity between terbium-labeled antibody and labeled FxxLF-motif peptide is established by co-activator recruitment to the AR-LBD (520:495 nm emission ratio after excitation at 340 nm). Data presented as mean ± SD of triplicates. (B) Chromatin immunoprecipitation analysis of AR in treated LNCaP-abl cells. Real-time PCR quantification of immunoprecipitated PSA enhancer is shown (R-1881, 10 nM; conjugate **1** or **2**, 1 μM). Data presented as mean + SD of triplicates. (C) Fluorescence-activated cell sorting analysis of treated LNCaP-abl cells (Veh., EtOH-treated cells; conjugate **1** or **2**, 1 μM).

contrast, conjugate **2** significantly decreased the cell population in the G_2/M and S phases and enhanced the G_0/G_1 cell population, relative to vehicle treatment. In addition, no increase in the apoptotic cell population was detected for cells treated in the presence of conjugate **1** or **2**. These results suggest that conjugate **2** induces cell-cycle arrest in the G_0/G_1 phase into the S phase transition, while conjugate **1** does not appear to induce growth arrest by influencing a particular stage of the cell cycle in LNCaP-abl cells.

Gene Expression Analysis. Recently, it has been shown that the AR is responsible for regulating a unique set of target genes in LNCaP-abl cells involved in cell-cycle progression including UBE2C, CCNA2, CKD1 and CDC20.[57] In particular, UBE2C has been shown to play a critical role in LNCaP-abl cell proliferation. Therefore, we examined if conjugates **1** and **2** were capable of affecting mRNA expression of these target genes in LNCaP-abl cells utilizing real-time PCR (Figure 5). Conjugates **1** and **2** modestly inhibit the expression of CCNA2 and CDC20, but not CDK1. In addition, conjugate **2**, but not **1**, reduced the expression of UBE2C. These results indicate that conjugates **1** and **2** differentially affect AR target gene expression in LNCaP-abl cells. This likely reflects the distinct mechanisms of AR antagonism exhibited by peptoid conjugates **1** and **2** (*vide supra*).

Genome-wide expression profiles of LNCaP-abl cells were obtained in the presence and absence of conjugates **1** or **2** and analyzed utilizing gene expression microarrays to identify global effects upon treatment in castrate-resistant prostate cancer cells. Relative to vehicle treatment, conjugate **1** affected 108 transcripts (10 up-regulated and 98 down-regulated) by at

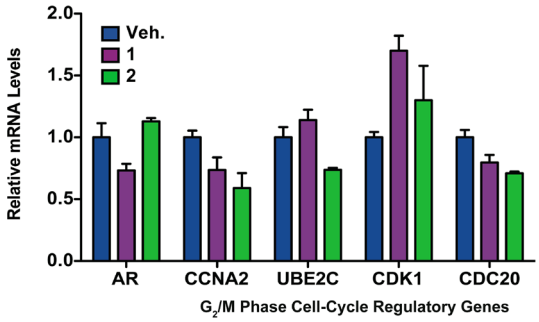

Figure 5. Relative mRNA expression of AR-target genes in treated LNCaP-abl cells quantified by real-time PCR (Veh., EtOH-treated cells; conjugate **1** or **2**, 10 μM). All data were normalized to the housekeeping gene GAPDH.[59]

least 2-fold ($P \leq 0.05$, Table 1). In contrast, a total of 1,086 transcripts (386 up-regulated and 700 down-regulated) were affected upon treatment with conjugate **2**, consistent with its ability to promote nuclear localization and co-activator recruitment. In addition, clustering analysis over all of the probed gene transcripts reveals that the expression profiles for LNCaP-abl cells treated with either conjugate **1** or **2** are distinct (Figure 6A and Supplementary Figure 5). Studies have shown that AR antagonists can alter the expression of androgen-induced genes, such as FKBP5, KLK3 (PSA), and AMIGO2.[5,56] In the presence of either conjugate **1** or **2**, we observe variations in expression of these genes. In comparing expression profiles of LNCaP-abl cells activated with hormone (DHT) or in a

dx.doi.org/10.1021/cb300332w | *ACS Chem. Biol.* 2012, 7, 1693–1701

Table 1. Number of Gene Transcripts Affected by Divalent Peptoid Conjugates 1 and 2 Relative to Vehicle Treatment ($P \leq 0.05$)

conjugate	up-regulated (fold change ≥ 1.5)	down-regulated (fold change ≤ −1.5)	up-regulated (fold change ≥ 2.0)	down-regulated (fold change ≤ −2.0)
1	89	247	10	98
2	998	1,545	386	700

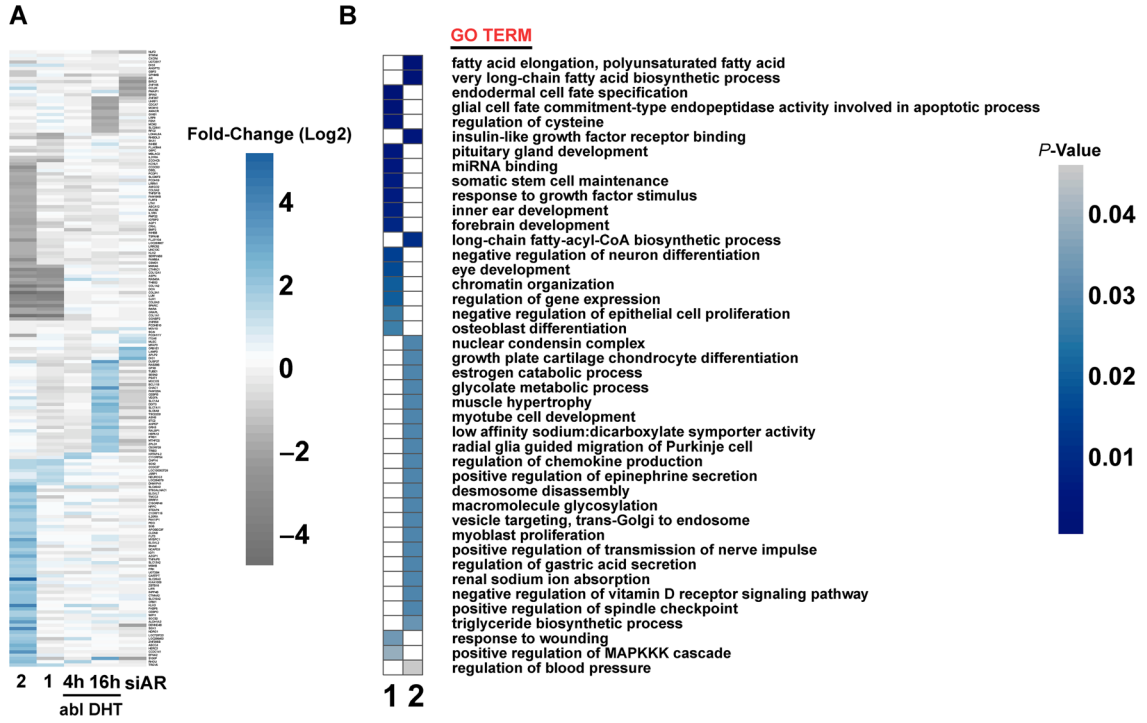

Figure 6. Conjugates **1** and **2** differentially effect gene expression of LNCaP-abl cells. (A) Clustering analysis of treated LNCaP-abl cells (conjugate **1** and **2** are compared to hormone-activated (DHT) and basal AR activity (siAR) states). Blue represents up-regulated genes, and gray indicates down-regulated genes, as specified by the scale color bar (fold-change). See also Supplementary Figure 5 for an expanded version. (B) Gene ontology (GO) enrichment analysis of treated LNCaP-abl cells (Veh., EtOH-treated cells; conjugate **1** or **2** (shown relative to Veh. treatment), 1 μM). Heat map showing enrichment score values for GO terms meeting the combined threshold ($P \leq 0.05$). Dark blue represents highly enriched GO terms, and light blue indicates depletion of the GO term from the indicated gene set, as specified by the scale color bar.

basal AR activity state (siAR), conjugates **1** and **2** can be clearly distinguished (GEO accession number GSE11428).[57]

To gain an overview of the biological processes that conjugate **1** or **2** may modulate, gene ontology (GO) enrichment analysis was performed. Enrichment scores elicited by conjugate **1** or **2** for genes up- or down-regulated by at least 3-fold ($P \leq 0.05$) reveal they are distinct, confirming that genome-wide expression is differentially affected by treatment with either conjugate **1** or **2** in LNCaP-abl cells (Figure 6B). The contrasting patterns in the gene expression and gene ontology enrichment profiles are consistent with conjugate **1** and **2** antagonizing the AR through different mechanisms of action.

To address the issue of potency, conjugates **1** and **2** were examined for their ability to induce AR-mediated transcriptional activation. We used a LNCaP cell line (androgen-dependent) that stably expresses the AR-responsive luciferase reporter gene under the probasin promoter (the rat homologue of PSA).[58] These cells, termed LB1-luc, were treated with conjugates **1** or **2** to a final concentration of 100 nM or 1 μM for 24 h, and AR-mediated transcriptional activation was measured.[22] Conjugates **1** and **2** fail to activate AR-mediated transcriptional activation at a concentration of 100 nM (Supplementary Figure 6) but activate AR at 1 μM.[22] These data, in combination with cell proliferation data (analyzed at 3 different concentrations in LNCaP-abl cells) and competitive binding data previously reported,[22] reveal that conjugates **1** and **2** are acting in distinctly different manners and that functional variations are not attributable to testing at a concentration for which one compound is more active.

There are currently no curative treatment regimens available for castrate-resistant prostate cancer, creating an urgent need to identify new therapeutic agents that modulate AR activity through unique mechanisms of action. Furthermore, the development of AR modulators that possess distinct mechanisms of AR antagonism has the potential advantage of circumventing drug resistance in AR pharmacology. The ability to mitigate AR nuclear function, thus preventing binding interactions between DNA and co-activator proteins, may address unmet clinical needs for castrate-resistant prostate cancer.

Conclusion. This study focuses on understanding the mechanisms by which a linear and a cyclic divalent peptoid conjugate exhibit their potent anti-proliferative properties in LNCaP-abl cells, a model of castrate-resistant prostate cancer. The linear conjugate competitively blocks AR action by inhibiting DNA binding. In addition, the linear conjugate does not promote AR nuclear localization or co-activator

dx.doi.org/10.1021/cb300332w | ACS Chem. Biol. 2012, 7, 1693−1701

binding. In contrast, the cyclic conjugate evokes nuclear localization and induces cell-cycle arrest despite its inability to compete against endogenous ligand for binding to AR *in vitro*, providing an alternative approach to inhibit AR activity with the potential to circumvent drug resistance. Genome-wide expression and gene ontology enrichment analysis reveals that different gene transcripts and biological processes are affected by treatment with the linear or cyclic conjugate. Additional macromolecular structural analysis and modeling will be important to provide further insight into the mechanism of action for these conjugates. Future studies will explore the molecular interactions underlying AR antagonism and evaluate the effects of divalent ethisterone peptoid conjugates *in vivo*.

METHODS

Peptoid Synthesis and Characterization. General synthesis and characterization methods for peptoid conjugates **1** and **2** were similar to those reported previously.[22]

Time Resolved Fluorescence Resonance Energy Transfer. LanthaScreen TR-FRET Androgen Receptor Co-activator Assay (Invitrogen) was used according to the manufacturer's instructions. Assay samples were prepared in triplicate on 384-well plates (Corning no. 3676) as recommended by the manufacturer and incubated at 25 °C for 2 h before data collection. The fluorescence emission values at 520 and 495 nm, evaluated using excitation at 340 nm, were obtained using a SpectraMax M5 plate reader (Molecular Devices) and SoftMax Pro software. All data were processed using GraphPad Prism.

Cell Culture. All cell lines were maintained at 5% CO_2 in a 37 °C incubator and cultured in appropriate media (refer to assay for conditions). Typically, cells were grown on 10 cm tissue-culture dishes (BD Falcon) to approximately 80% confluence before subculture.

Protein Expression. LNCaP-abl cells were grown on 10 cm culture dishes (BD Falcon) in RPMI media supplemented with 10% fetal bovine serum (FBS), 1% L-glutamine (L-Gln) and 1% penicillin/streptomycin (PS). Cells were treated with conjugate **1** or **2** to a final concentration of 1 μM and allowed to incubate at 37 °C for 48−72 h. Following treatment, cells were harvested in PBS buffer, centrifuged and lysed with RIPA buffer (10 mM Tris (pH 8.0), 1 mM EDTA (pH 8.0), 140 mM NaCl, 5% glycerol, 0.1% Deoxycholate, 0.1% SDS, and 1% Triton X-100) containing 1 mM Na_3VO_4 and 1X protease inhibitor to obtain cellular extracts. Protein concentration was quantified by a standard colorimetric Bradford assay (Bio-Rad), and samples were subjected to SDS-PAGE (25 μg protein well^{-1}). The separated proteins were then transferred onto Immobilon membranes (Millipore) and probed with anti-AR (441, Santa Cruz Biotechnology) or anti-tubulin (Covance) primary antibodies followed by horseradish peroxidase-conjugated goat anti-mouse or anti-rabbit IgG secondary antibodies.

Cellular Localization. HEK293 cells were seeded on pretreated (poly-D-lysine) 8-well chamber slides (Nunc) at a density of 3.0×10^4 cells well^{-1} in DMEM media supplemented with 10% FBS, 1% L-Gln, and 1% PS. Following attachment, cells were transfected with an AR fluorescent protein hybrid (kind gift of Jeremy Jones, City of Hope, CA) and starved in DMEM media supplemented with 10% charcoal-stripped FBS for 72 h. Following starvation, cells were treated with peptoid conjugate **1** or **2** (1 μM) or DHT (1 nM) and allowed to incubate at 37 °C for 4 h. Cells were fixed for 20 min in PBS containing 4% formaldehyde and stained with DAPI mounting solution. Images were analyzed and acquired using a Leica TCS SP5 II Confocal Microscope.

Chromatin Immunoprecipitation. LNCaP-abl cells were grown on 10 cm culture dishes (BD Falcon) to approximately 70% confluence in RPMI media supplemented with 10% charcoal-stripped FBS, 1% L-Gln, and 1% PS. Following attachment, cells were treated with conjugates **1** or **2** (1 μM) plus R-1881 (10 nM) and allowed to incubate at 37 °C for 4 or 16 h. Following treatment, proteins were double cross-linked with DSP (Pierce) for 20 min and 1% formalin for 10 min. Cells were lysed, and nuclei were collected, lysed in buffer (1% SDS, 50 mM Tris-HCl (pH 8.0), 10 mM EDTA), and sonicated for 12 min (30 s on, 30 s off) utilizing a Bioruptor sonicator (Diagenode, model XL). Sonicated lysates were precleared for 2 h with Protein A/G agarose beads blocked with salmon sperm DNA (Millipore). Supernatants were then incubated overnight with a mixture of antibodies to AR (2 μg AR-441 and 2 μg AR-N20, Santa Cruz Biotechnology). Control ChIP was concurrently performed with the same quantity of normal mouse and rabbit IgG sera. Immunocomplexes were then washed and cross-linking was reversed. DNA was isolated with a PCR purification kit (Qiagen) according to the manufacturer's instructions, and real-time PCR was performed. Relative enrichment of indicated genomic locus was calculated as a percentage of 4% input normalized to IgG. All data were processed using GraphPad Prism.

Flow Cytometry. LNCaP-abl cells were grown on 10 cm culture dishes (BD Falcon) to approximately 70% confluence in RPMI media supplemented with 10% charcoal-stripped FBS, 1% L-Gln, and 1% PS. Cells were then treated with conjugate **1** or **2** to a final concentration of 1 μM and allowed to incubate at 37 °C for 48 h. Following treatment, cells were fixed and suspended in 2 mL of 1:3 HBSS:Phosphate-Citrate Buffer (pH 8.0) containing 0.1% Triton X-100. Cells were centrifuged (2,000 rpm for 5 min) and suspended in 1 mL of propidium-iodide solution (1 mg propidium iodine, 10 mg EDTA, 250 μL Igepal, and 2.2 μg μL^{-1} RNAase in 50 mL of PBS). Cells were then harvested for cell-cycle analysis by filtration (CellTrics, 100 μm) into conical tubes (Falcon) and analyzed by flow cytometry (Becton-Dickinson FACScalibur). All data were analyzed using FlowJo software.

AR Target Gene Expression. LNCaP-abl cells were grown on 6 cm culture dishes (BD Falcon) at a density of approximately 1.0×10^6 cells well^{-1} in charcoal-stripped RPMI supplemented with 10% FBS, 1% L-Glu, and 1% PS. Cells were then treated with conjugate **1** or **2** to a final concentration of 10 μM and allowed to incubate at 37 °C for 24 h. Following treatment, cells were harvested, and RNA was extracted utilizing the RNeasy mini kit (Qiagen) according to the manufacturer's instructions. RNA concentration was quantified by UV absorbance *via* NanoDrop (Thermo-Scientific). Complementary DNA was then prepared by PCR (MJ Research PTC-200 Thermo Cycler) and relative mRNA levels for G_2/M-phase cell-cycle regulatory genes were determined by real-time PCR (Bio-Rad MyiQ) using the SYBR Green PCR kit (Applied Biosystems) according to the manufacturer's instructions. All data were processed using GraphPad Prism.

Microarray Analysis. LNCaP-abl cells were grown on 10 cm culture dishes (BD Falcon) to approximately 70% confluence in RPMI media supplemented with 10% charcoal-stripped FBS, 1% L-Gln, and 1% PS. Cells were then treated with conjugate **1** or **2** to a final concentration of 1 μM and allowed to incubate at 37 °C for 24 h. Following treatment, cells were harvested, and RNA was extracted and quantified as described above. The final RNA concentration for each sample was >1 μg μL^{-1}. Microarray experiments were carried out at the Memorial Sloan-Kettering Cancer Center Genomics Core Facility using Affymetrix Human Genome U133 plus 2.0 expression arrays. Normalization of the raw data was conducted using R BioConductor and the "affy" data processing package.[60,61]

AR-Mediated Transcription Assay. LB1-luc cells were seeded in triplicate on 24-well plates (Corning) at a density of approximately 7.5×10^4 cells/well in RPMI media supplemented with 10% fetal bovine serum (FBS), 1% L-Gln, and 1% PS. Following attachment, cells were starved for 48 h with RPMI media supplemented with 10% charcoal-stripped FBS, treated with conjugates to a final concentration of 100 nM, and incubated at 37 °C for 24 h. Following incubation, cells were washed with PBS and lysed in 1X luciferase cell culture lysis reagent (Promega) according to the manufacturer's instructions. Luciferase activity was quantified in a reaction mixture containing 10 μL of cell lysate and 50 μL of luciferase assay reagent (Promega) using a microplate luminometer (LMax). All data were processed using GraphPad Prism.

■ ASSOCIATED CONTENT

Supporting Information

Control experiments and expanded figures. This material is available free of charge via the Internet at http://pubs.acs.org.

Accession Codes

Gene Expression Omnibus accession number (GSE37796)

■ AUTHOR INFORMATION

Corresponding Author

*E-mail: kent@nyu.edu.

Notes

The authors declare no competing financial interest.

■ ACKNOWLEDGMENTS

This work was financially supported by the NSF (CHE-1152317 to K. Kirshenbaum) and the NIH (Research Facilities Improvement Grant C060RR-165720), and CA11226 (S. K. Logan). Supported in part by grant UL1 TR000038 from the National Center for the Advancement of Translational Science (NCATS), National Institutes of Health. We thank J. Jones (City of Hope, CA) for the AR-fluorescent fusion protein constructs and the NYULMC flow cytometry and microscopy core facilities. E. Lee thanks NYSTEM Training Grant Contract no. C026880 for support.

■ REFERENCES

(1) Meimetis, L. G., Williams, D. E., Mawji, N. R., Banuelos, C. A., Lal, A. A., Park, J. J., Tien, A. H., Fernandez, J. G., de Voogd, N. J., Sadar, M. D., and Andersen, R. J. (2011) Niphatenones, Glycerol Ethers from the Sponge Niphates Digitalis Block Androgen Receptor Transcriptional Activity in Prostate Cancer Cells: Structure Elucidation, Synthesis, and Biological Activity. *J. Med. Chem. 55*, 503−514.

(2) Hodgson, M. C., Astapova, I., Hollenberg, A. N., and Balk, S. P. (2007) Activity of Androgen Receptor Antagonist Bicalutamide in Prostate Cancer Cells is Independent of NCoR and SMRT Corepressors. *Cancer Res. 67*, 8388−8395.

(3) Lassi, K., and Dawson, N. A. (2009) Emerging Therapies in Castrate-Resistant Prostate Cancer. *Curr. Opin. Oncol. 21*, 260−265.

(4) Rennie, P. S., and Nelson, C. C. (1998) Epigenetic Mechanisms for Progression of Prostate Cancer. *Cancer Metastasis Rev. 17*, 401−409.

(5) Clegg, N. J., Wongvipat, J., Tran, C., Ouk, S., Dilhas, A., Joseph, J., Chen, Y., Grillot, K., Bischoff, E. D., Cai, L., Aparicio, A., Dorow, S., Arora, V., Shao, G., Qian, J., Zhao, H., Yang, G., Cao, C., Sensintaffar, J., Wasielewska, T., Herbert, M. R., Bonnefous, C., Darimont, B., Scher, H. I., Smith-Jones, P. M., Klang, M., Smith, N. D., de Stanchina, E., Wu, N., Ouerfelli, O., Rix, P., Heyman, R., Jung, M. E., Sawyers, C. L., and Hager, J. H. (2012) ARN-509: A Novel Anti-Androgen for Prostate Cancer Treatment. *Cancer Res. 15*, 1494−1503.

(6) Bhasin, S., Cunningham, G. R., Hayes, F. J., Matsumoto, A. M., Snyder, P. J., Swerdloff, R. S., and Montori, V. M. (2010) Testosterone Therapy in Men with Androgen Deficiency Syndromes: An Endocrine Society Clinical Practice Guideline. *J. Clin. Endocrinol. Metab. 95*, 2536−2559.

(7) Gelmann, E. P. (2002) Molecular Biology of the Androgen Receptor. *J. Clin. Oncol. 20*, 3001−3015.

(8) Edwards, J., Krishna, N. S., Grigor, K. M., and Bartlett, J. M. S. (2003) Androgen Receptor Gene Amplification and Protein Expression in Hormone Refractory Prostate Cancer. *Br. J. Cancer 89*, 552−556.

(9) Georget, V., Terouanne, B. A., Nicolas, J.-C., and Sultan, C. (2002) Mechanism of Antiandrogen Action: Key Role of Hsp90 in Conformational Change and Transcriptional Activity of the Androgen Receptor. *Biochemistry 41*, 11824−11831.

(10) Heinlein, C. A., and Chang, C. (2004) Androgen Receptor in Prostate Cancer. *Endocr. Rev. 25*, 276−308.

(11) Schaufele, F., Carbonell, X., Guerbadot, M., Borngraeber, S., Chapman, M. S., Ma, A. A. K., Miner, J. N., and Diamond, M. I. (2005) The Structural Basis of Androgen Receptor Activation: Intramolecular and Intermolecular Amino-Carboxy Interactions. *Proc. Natl. Acad. Sci. U.S.A. 102*, 9802−9807.

(12) Gioeli, D., Ficarro, S. B., Kwiek, J. J., Aaronson, D., Hancock, M., Catling, A. D., White, F. M., Christian, R. E., Settlage, R. E., Shabanowitz, J., Hunt, D. F., and Weber, M. J. (2002) Androgen Receptor Phosphorylation. Regulation and Identification of the Phosphorylation Sites. *J. Biol. Chem. 277*, 29304−29314.

(13) Shaffer, P. L., Jivan, A., Dollins, D. E., Claessens, F., and Gewirth, D. T. (2004) Structural Basis of Androgen Receptor Binding to Selective Androgen Response Elements. *Proc. Natl. Acad. Sci. U.S.A. 101*, 4758−4763.

(14) He, B., Minges, J. T., Lee, L. W., and Wilson, E. M. (2002) The FXXLF Motif Mediates Androgen Receptor-Specific Interactions with Coregulators. *J. Biol. Chem. 277*, 10226−10235.

(15) McGinley, P. L., and Koh, J. T. (2007) Circumventing Anti-Androgen Resistance by Molecular Design. *J. Am. Chem. Soc. 129*, 3822−3823.

(16) Tran, C., Ouk, S., Clegg, N. J., Chen, Y., Watson, P. A., Arora, V., Wongvipat, J., Smith-Jones, P. M., Yoo, D., Kwon, A., Wasielewska, T., Welsbie, D., Chen, C. D., Higano, C. S., Beer, T. M., Hung, D. T., Scher, H. I., Jung, M. E., and Sawyers, C. L. (2009) Development of a Second-Generation Antiandrogen for Treatment of Advanced Prostate Cancer. *Science 324*, 787−790.

(17) Chen, C. D., Welsbie, D. S., Tran, C., Baek, S. H., Chen, R., Vessella, R., Rosenfeld, M. G., and Sawyers, C. L. (2004) Molecular Determinants of Resistance to Antiandrogen Therapy. *Nat. Med. 10*, 33−39.

(18) Andersen, R. J., Mawji, N. R., Wang, J., Wang, G., Haile, S., Myung, J.-K., Watt, K., Tam, T., Yang, Y. C., Banuelos, C. A., Williams, D. E., McEwan, I. J., Wang, Y., and Sadar, M. D. (2010) Regression of Castrate-Recurrent Prostate Cancer by a Small-Molecule Inhibitor of the Amino-Terminus Domain of the Androgen Receptor. *Cancer Cell 17*, 535−546.

(19) Dubrovska, A., Kim, C., Elliott, J., Shen, W., Kuo, T.-H., Koo, D.-I., Li, C., Tuntland, T., Chang, J., Groessl, T., Wu, X., Gorney, V., Ramirez-Montagut, T., Spiegel, D. A., Cho, C. Y., and Schultz, P. G. (2011) A Chemically Induced Vaccine Strategy for Prostate Cancer. *ACS Chem. Biol. 6*, 1223−1231.

(20) Estébanez-Perpiñá, E., Arnold, L. A., Nguyen, P., Rodrigues, E. D., Mar, E., Bateman, R., Pallai, P., Shokat, K. M., Baxter, J. D., Guy, R. K., Webb, P., and Fletterick, R. J. (2007) A Surface on the Androgen Receptor that Allosterically Regulates Coactivator Binding. *Proc. Natl. Acad. Sci. U.S.A. 104*, 16074−16079.

(21) Buzón, V., Carbó, L. R., Estruch, S. B., Fletterick, R. J., and Estébanez-Perpiñá, E. (2012) A Conserved Surface on the Ligand Binding Domain of Nuclear Receptors for Allosteric Control. *Mol. Cell. Endocrinol. 348*, 394−402.

(22) Levine, P. M., Imberg, K., Garabedian, M. J., and Kirshenbaum, K. (2012) Multivalent Peptidomimetic Conjugates: A Versatile Platform for Modulating Androgen Receptor Activity. *J. Am. Chem. Soc. 134*, 6912−6915.

(23) Kiessling, L. L., Gestwicki, J. E., and Strong, L. E. (2000) Synthetic Multivalent Ligands in the Exploration of Cell-Surface Interactions. *Curr. Opin. Chem. Biol. 4*, 696−703.

(24) Childs-Disney, J. L., Tsitovich, P. B., and Disney, M. D. (2011) Using Modularly Assembled Ligands to Bind RNA Internal Loops Separated by Different Distances. *ChemBioChem 12*, 2143−2146.

(25) Englund, E. A., Wang, D., Fujigaki, H., Sakai, H., Micklitsch, C. M., Ghirlando, R., Martin-Manso, G., Pendrak, M. L., Roberts, D. D., Durell, S. R., and Appella, D. H. (2012) Programmable Multivalent Display of Receptor Ligands Using Peptide Nucleic Acid Nano-scaffolds. *Nat. Commun. 3*, 614.

(26) Bryson, D. I., Zhang, W., McLendon, P. M., Reineke, T. M., and Santos, W. L. (2011) Toward Targeting RNA Structure: Branched

Peptides as Cell-Permeable Ligands to TAR RNA. *ACS Chem. Biol. 7*, 210−217.
(27) Fournel, S., Wieckowski, S., Sun, W., Trouche, N., Dumortier, H., Bianco, A., Chaloin, O., Habib, M., Peter, J.-C., Schneider, P., Vray, B., Toes, R. E., Offringa, R., Melief, C. J. M., Hoebeke, J., and Guichard, G. (2005) C3-Symmetric Peptide Scaffolds are Functional Mimetics of Trimeric CD40L. *Nat. Chem. Biol. 1*, 377−382.
(28) Kitov, P. I., Sadowska, J. M., Mulvey, G., Armstrong, G. D., Ling, H., Pannu, N. S., Read, R. J., and Bundle, D. R. (2000) Shiga-Like Toxins are Neutralized by Tailored Multivalent Carbohydrate Ligands. *Nature 403*, 669−672.
(29) Lee, J., Udugamasooriya, D. G., Lim, H.-S., and Kodadek, T. (2010) Potent and Selective Photo-Inactivation of Proteins with Peptoid-Ruthenium Conjugates. *Nat. Chem. Biol. 6*, 258−260.
(30) Raskatov, J. A., Hargrove, A. E., So, A. Y., and Dervan, P. B. (2012) Pharmacokinetics of Py-Im Polyamides Depend on Architecture: Cyclic versus Linear. *J. Am. Chem. Soc. 134*, 7995−7999.
(31) Holub, J. M., Garabedian, M. J., and Kirshenbaum, K. (2011) Modulation of Human Estrogen α Receptor Activity by Multivalent Estradiol-Peptidomimetic Conjugates. *Mol. BioSyst. 7*, 337−345.
(32) Yuasa, H., Honma, H., Hashimoto, H., Tsunooka, M., and Kojima-Aikawa, K. (2007) Pentamer is the Minimum Structure for Oligomannosylpeptoids to Bind to Concanavalin A. *Bioorg. Med. Chem. Lett. 17*, 5274−5278.
(33) Lee, M. M., Pushechnikov, A., and Disney, M. D. (2009) Rational and Modular Design of Potent Ligands Targeting the RNA That Causes Myotonic Dystrophy 2. *ACS Chem. Biol. 4*, 345−355.
(34) Miller, S. M., Simon, R. J., Ng, S., Zuckermann, R. N., Kerr, J. M., and Moos, W. H. (1995) Comparison of the Proteolytic Susceptibilities of Homologous L-Amino Acid, D-Amino Acid, and *N*-substituted Glycine Peptide and Peptoid Oligomers. *Drug Dev. Res. 35*, 20−32.
(35) Tan, N. C., Yu, P., Kwon, Y.-U., and Kodadek, T. (2008) High-Throughput Evaluation of Relative Cell Permeability Between Peptoids and Peptides. *Bioorg. Med. Chem. 16*, 5853−5861.
(36) Maayan, G., Ward, M. D., and Kirshenbaum, K. (2009) Folded Biomimetic Oligomers for Enantioselective Catalysis. *Proc. Natl. Acad. Sci. U.S.A. 106*, 13679−13684.
(37) Maayan, G., Ward, M. D., and Kirshenbaum, K. (2009) Metallopeptoids. *Chem. Commun.*, 56−58.
(38) Huang, M. L., Shin, S. B. Y., Benson, M. A., Torres, V. J., and Kirshenbaum, K. (2012) A Comparison of Linear and Cyclic Peptoid Oligomers as Potent Antimicrobial Agents. *ChemMedChem 7*, 114−122.
(39) Fowler, S. A., and Blackwell, H. E. (2009) Structure-Function Relationships in Peptoids: Recent Advances Toward Deciphering the Structural Requirements for Biological Function. *Org. Biomol. Chem. 7*, 1508−1524.
(40) Chongsiriwatana, N. P., Patch, J. A., Czyzewski, A. M., Dohm, M. T., Ivankin, A., Gidalevitz, D., Zuckermann, R. N., and Barron, A. E. (2008) Peptoids that Mimic the Structure, Function, and Mechanism of Helical Antimicrobial Peptides. *Proc. Natl. Acad. Sci. U.S.A. 105*, 2794−2799.
(41) Murphy, J. E., Uno, T., Hamer, J. D., Cohen, F. E., Dwarki, V., and Zuckermann, R. N. (1998) A Combinatorial Approach to the Discovery of Efficient Cationic Peptoid Reagents for Gene Delivery. *Proc. Natl. Acad. Sci. U.S.A. 95*, 1517−1522.
(42) Udugamasooriya, D. G., Dineen, S. P., Brekken, R. A., and Kodadek, T. (2008) A Peptoid "Antibody Surrogate" that Antagonizes VEGF Receptor 2 Activity. *J. Am. Chem. Soc. 130*, 5744−5752.
(43) Zuckermann, R. N., Kerr, J. M., Kent, S. B. H., and Moos, W. H. (1992) Efficient Method for the Preparation of Peptoids [oligo(*N*-substituted glycines)] by Submonomer Solid-Phase Synthesis. *J. Am. Chem. Soc. 114*, 10646−10647.
(44) Lee, Y., and Sampson, N. S. (2006) Romping the Cellular Landscape: Linear Scaffolds for Molecular Recognition. *Curr. Opin. Struct. Biol. 16*, 544−550.
(45) Yoo, B., Shin, S. B. Y., Huang, M. L., and Kirshenbaum, K. (2010) Peptoid Macrocycles: Making the Rounds with Peptidomimetic Oligomers. *Chem.—Eur. J. 16*, 5528−5537.
(46) Holub, J. M., Garabedian, M. J., and Kirshenbaum, K. (2007) Peptoids on Steroids: Precise Multivalent Estradiol−Peptidomimetic Conjugates Generated *via* Azide−Alkyne [3 + 2] Cycloaddition Reactions. *QSAR Comb. Sci. 26*, 1175−1180.
(47) Shin, S. B. Y., Yoo, B., Todaro, L. J., and Kirshenbaum, K. (2007) Cyclic Peptoids. *J. Am. Chem. Soc. 129*, 3218−3225.
(48) Holub, J. M., and Kirshenbaum, K. (2010) Tricks with Clicks: Modification of Peptidomimetic Oligomers *via* Copper-Catalyzed Azide-Alkyne [3 + 2] Cycloaddition. *Chem. Soc. Rev. 39*, 1325−1337.
(49) Rezai, T., Bock, J. E., Zhou, M. V., Kalyanaraman, C., Lokey, R. S., and Jacobson, M. P. (2006) Conformational Flexibility, Internal Hydrogen Bonding, and Passive Membrane Permeability: Successful in Silico Prediction of the Relative Permeabilities of Cyclic Peptides. *J. Am. Chem. Soc. 128*, 14073−14080.
(50) Rezai, T., Yu, B., Millhauser, G. L., Jacobson, M. P., and Lokey, R. S. (2006) Testing the Conformational Hypothesis of Passive Membrane Permeability Using Synthetic Cyclic Peptide Diastereomers. *J. Am. Chem. Soc. 128*, 2510−2511.
(51) Culig, Z., Hoffmann, J., Erdel, M., Eder, I. E., Hobisch, A., Hittmair, A., Bartsch, G., Utermann, G., Schneider, M. R., Parczyk, K., and Klocker, H. (1999) Switch from Antagonist to Agonist of the Androgen Receptor Blocker Bicalutamide is Associated with Prostate Tumour Progression in a New Model System. *Br. J. Cancer 81*, 242−251.
(52) Waller, A., Sharrard, R., Berthon, P., and Maitland, N. (2000) Androgen Receptor Localisation and Turnover in Human Prostate Epithelium Treated with the Antiandrogen, Casodex. *J. Mol. Endocrinol. 24*, 339−351.
(53) Jones, J. O., An, W. F., and Diamond, M. I. (2009) AR Inhibitors Identified by High-Throughput Microscopy Detection of Conformational Change and Subcellular Localization. *ACS Chem. Biol. 4*, 199−208.
(54) Ozers, M. S., Marks, B. D., Gowda, K., Kupcho, K. R., Ervin, K. M., De Rosier, T., Qadir, N., Eliason, H. C., Riddle, S. M., and Shekhani, M. S. (2006) The Androgen Receptor T877A Mutant Recruits LxxLL and FxxLF Peptides Differently than Wild-Type Androgen Receptor in a Time-Resolved Fluorescence Resonance Energy Transfer Assay. *Biochemistry 46*, 683−695.
(55) Osguthorpe, D. J., and Hagler, A. T. (2011) Mechanism of Androgen Receptor Antagonism by Bicalutamide in the Treatment of Prostate Cancer. *Biochemistry 50*, 4105−4113.
(56) Nickols, N. G., and Dervan, P. B. (2007) Suppression of Androgen Receptor-Mediated Gene Expression by a Sequence-Specific DNA-Binding Polyamide. *Proc. Natl. Acad. Sci. U.S.A. 104*, 10418−10423.
(57) Wang, Q., Li, W., Zhang, Y., Yuan, X., Xu, K., Yu, J., Chen, Z., Beroukhim, R., Wang, H., Lupien, M., Wu, T., Regan, M. M., Meyer, C. A., Carroll, J. S., Manrai, A. K., Janne, O. A., Balk, S. P., Mehra, R., Han, B., Chinnaiyan, A. M., Rubin, M. A., True, L., Fiorentino, M., Fiore, C., Loda, M., Kantoff, P. W., Liu, X. S., and Brown, M. (2009) Androgen Receptor Regulates a Distinct Transcription Program in Androgen-Independent Prostate Cancer. *Cell 138*, 245−256.
(58) Zhang, J., Gao, N., DeGraff, D. J., Yu, X., Sun, Q., Case, T. C., Kasper, S., and Matusik, R. J. (2010) Characterization of Cis Elements of the Probasin Promoter Necessary for Prostate-Specific Gene Expression. *Prostate 70*, 934−951.
(59) Barber, R. D., Harmer, D. W., Coleman, R. A., and Clark, B. J. (2005) GAPDH as a Housekeeping Gene: Analysis of GAPDH mRNA Expression in a Panel of 72 Human Tissues. *Physiol. Genomics 21*, 389−395.
(60) Gautier, L., Cope, L., Bolstad, B. M., and Irizarry, R. A. (2004) Affy−Analysis of Affymetrix GeneChip Data at the Probe Level. *Bioinformatics 20*, 307−315.
(61) Gentleman, R., Carey, V., Bates, D., Bolstad, B., Dettling, M., Dudoit, S., Ellis, B., Gautier, L., Ge, Y., Gentry, J., Hornik, K., Hothorn, T., Huber, W., Iacus, S., Irizarry, R., Leisch, F., Li, C., Maechler, M.,

Rossini, A., Sawitzki, G., Smith, C., Smyth, G., Tierney, L., Yang, J., and Zhang, J. (2004) Bioconductor: Open Software Development for Computational Biology and Bioinformatics. *Genome Biol. 5*, R80.